Competition between Shear-Melting and Taylor Instabilities in Colloidal Crystals

Jean-Marc di Meglio,[(1),(2),(a)] D. A. Weitz,[(1)] and P. M. Chaikin[(1),(2)]
[(1)]*Exxon Research and Engineering Company, Annandale, New Jersey 08801*
[(2)]*Department of Physics, University of Pennsylvania, Philadelphia, Pennsylvania 19104*
(Received 29 October 1986)

We study the onset of the Taylor instability for colloidal crystals in a narrow-gap Couette cell. There is a natural competition between the radial flow required for Taylor rolls and the resistance to such motion caused by the anisotropy of the flowing solid. A new, combined Taylor–shear-melting instability is found at rotation rates above those expected for the formation of rolls, but below the shear rate required for shear melting in the absence of the Taylor instability. The control parameter for the shear-melting transition appears to be a critical shear stress rather than the shear rate.

PACS numbers: 62.20.−x, 47.20.−k, 64.70.Dv

Colloidal crystals, comprised of charged polystyrene spheres in aqueous suspension, or "polyballs," are good model systems for studying the equilibrium and dynamic properties of conventional solid and liquids because of the controllability of both the interparticle interactions and the particle density.[1,2] They also exhibit phenomena previously unobserved in other materials. Recent interest has centered on the shear-melting transition, which is not as yet fully understood.[3–6] Primarily because of the low particle density, $\sim 10^{13}/\mathrm{cm}^3$, the elastic constants of colloidal crystals are very small,[7] $\sim 1-1000$ dyn/cm^2. Thus colloidal crystals can flow easily under a relatively small shear stress. However, their rheological behavior is both highly non-Newtonian and anisotropic. As the shear is increased, a transition, or series of transitions, is observed. These are characterized by a loss of the opalesence caused by Bragg scattering from the crystalline phase,[3–5] and a jump in the viscosity.[4,8] Most models for this solid-to-liquid shear-melting transition assume that it is controlled solely by the local shear rate.[3,5,6]

In this Letter, we discuss the onset of the Taylor instability in Couette flow of colloidal crystals. The aim of the experiments was twofold, both to study the shear-melting transition in the presence of stresses aside from simple shear, and to study the effect of non-Newtonian, anisotropic fluid on the Taylor instability.[9] The anisotropy arises when the colloidal crystal is subjected to sufficient shear to cause it to flow, but insufficient to cause it to undergo shear melting. The flowing solid can be described either as a sliding of ordered planes,[5] or by dislocation motion.[10,11] In either case, one expects a highly anisotropic response to an incremental stress, with a lower effective viscosity along the direction of the flow than along the direction of the velocity gradient. The onset of the Taylor instability and the formation of rolls is induced by the centrifugal forces which cause an additional, radial motion in the direction of the velocity gradient. For colloidal crystals this leads to a natural competition between these forces and the tendency of the flowing solid to maintain its density wave and rigidity in this direction. Also, the centrifugal forces can induce additional stresses, resulting in a possible modification of the shear-melting transition. Thus one might expect the Taylor instability to occur at a critical Taylor number dictated by some effective viscosity for the non-Newtonian, flowing solid, with the crystal planes aligned with the rolls. Alternatively, if the solid is sufficiently rigid one might expect suppression of the Taylor rolls until the shear-melting transition, when the fluid becomes more isotropic.

Instead the present experiments show that the Taylor instability and the shear-melting transition occur simultaneously. Furthermore, this new Taylor–shear-melting transition occurs at a critical rotation frequency considerably higher than expected for the Taylor instability, while the critical shear rate is substantially smaller than that expected for shear melting. This implies that the shear-melting transition is *not* controlled solely by the local shear rate, but depends on the actual flow pattern and the stresses generated. In fact, the experiments suggest that the shear melting is controlled by the shear stress rather than the shear rate.

The experiment was performed in a conventional narrow-gap Couette cell with inner radius $R = 4.765$ cm, gap $d = 0.315$ cm, and height ~ 20 cm. The colloidal sample consisted of polyballs 0.091 μm in diameter at 2.5% volume fraction. The geometry and polyball sample were chosen so that the onset of the Taylor instability would occur at a lower rotation rate than required to cause shear melting of the sample in contrast to a previous study.[12] In Fig. 1 we show the curve of shear stress versus shear rate for a typical sample used in this study. The measurement was made in a Zimm viscometer with a sufficiently small gap that the Taylor instability occurs at high shear rates and is not observed. Below 200 Hz the flowing solid shows a highly non-Newtonian behavior. The shear-melting transition is signaled by the rapid increase in stress σ at a shear rate $\dot{\gamma} \sim 260$ Hz. Above the transition, the liquid has a higher viscosity, ν, either

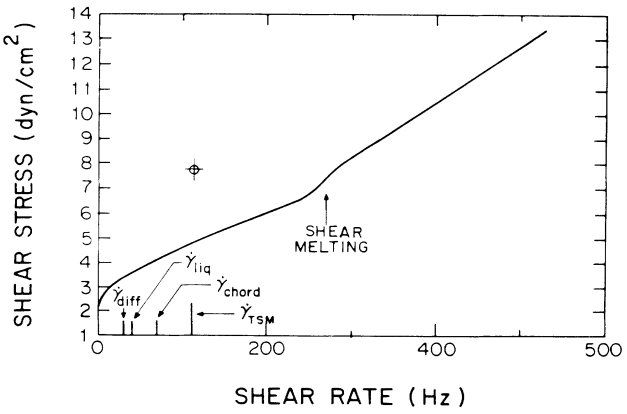

FIG. 1. Shear stress vs shear rate for a 2% volume fraction sample of 0.091-μm polyballs. The γ_i's are the predicted shear rates for Taylor roll onset from various criteria. Circled plus is the effective stress and actual rate at which the combined Taylor–shear-melting instability occurs.

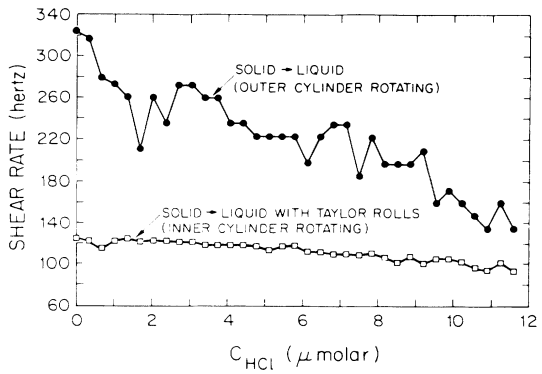

FIG. 2. Upper curve is the phase boundary between flowing solid and shear-melted liquid for outer-cylinder rotation. Lower curve is the phase boundary between flowing solid and shear-melted liquid with Taylor rolls for inner-cylinder rotation.

chordal ($\sigma/\dot{\gamma}$) or differential ($\partial\sigma/\partial\dot{\gamma}$), than the solid.

In our Couette cell the shear rate is approximately constant and is related to the angular velocity of the inner cylinder, Ω, by $\dot{\gamma}\sim\Omega R/d$. In narrow-gap geometry with only the inner cylinder rotating the Taylor number has the limiting form $T=\Omega^2Rd^3/\nu^2$.[9,13] The onset of the Taylor instability occurs at a critical value, $T_c\approx 1700$. Thus by determining the critical rotation rate, Ω_c, we can measure the critical shear rate, $\dot{\gamma}_c$, and infer an effective viscosity, ν_c, of the fluid at the onset of the Taylor instability. These are $\dot{\gamma}_c\approx 112$ Hz and $\nu_c\approx 0.07$ poise. It is instructive to compare these numbers with the results in Fig. 1 obtained from the Zimm viscometer. Taking $\nu_c\dot{\gamma}_c$ as $\sigma_c\approx 7.8$ dyn/cm^2, the effective shear stress at the instability, we have plotted $(\dot{\gamma}_c,\sigma_c)$ in Fig. 1.

By comparison, we can use different values of the viscosity together with the condition $T_c\approx 1700$ to determine the shear rate at which the Taylor instability alone might have been expected [i.e., we take $\dot{\gamma}_i=(T_c R\nu_i^2/d^5)^{1/2}$]. The expected $\dot{\gamma}$'s are shown on the abscissa of Fig. 1. If we use the differential viscosity of the shear-melted liquid, we obtain $\dot{\gamma}_{liq}$. If we require a form of self-consistency, then we must choose a shear rate which would give $T=1700$ using a viscosity at that shear rate. If we choose the chordal viscosity the result is $\dot{\gamma}_{chord}$. Similarly, with use of the differential viscosity the result is γ_{diff}. The actual shear rate at which the combined Taylor–shear-melting transition occurred, $\dot{\gamma}_c$, is higher than any rate expected for the Taylor instability. This indicates that the anisotropy of the flowing solid plays a crucial role in suppressing the Taylor instability. Furthermore, the sample undergoes shear melting at a considerably lower rate than that which would produce shear melting in the absence of the Taylor instability. This indicates that the shear rate is not the only control parameter for the shear-melting transition.

The most dramatic and direct proof that the Taylor instability has a profound effect on the shear-melting transition is provided by an experiment comparing the rate at which shear melting occurs, $\dot{\gamma}_{sm}$, for the same sample in the same Couette cell when either the inner or the outer cylinder was rotating. When the shear is established by rotation of the inner cylinder, the centrifugal forces induce the Taylor instability, while if the same shear is established by rotation of the outer cylinder, no instability occurs. The measured $\dot{\gamma}_{sm}$'s for each case are shown in Fig. 2 as a function of electrolyte concentration. The upper curve (plusses) represents the phase boundary between the shear-melted liquid and the flowing solid with the outer cylinder rotating and thus in the absence of destabilizing centrifugal forces. The lower curve (squares) marks the phase boundary between the flowing solid and the shear-melted liquid *with* Taylor rolls, for inner-cylinder rotation. As electrolyte was added to decrease the strength of the interparticle interactions, the critical rotation rate for shear melting with Taylor rolls remained considerably below that without Taylor rolls, until the samples melted in zero shear, at $\sim 12\,\mu M$ HCl.

With $T_c\approx 1700$, as appropriate for our geometry, the observed Ω_c for the combined Taylor–shear-melting transitions implies that the viscosity for the liquid phase just above the transitions is substantially higher than any viscosity measured for the samples (in either the solid or liquid states except at very low $\dot{\gamma}$), in the absence of the Taylor instability. This is indicated by the open circle corresponding to $(\dot{\gamma}_c,\sigma_c)$ in Fig. 1, which lies well above the stress-rate curve. To see whether such large viscosities, and concomitant shear stresses, exist in the presence of the Taylor rolls, we constructed an apparatus capable of measuring the shear stress in the wall of the Couette

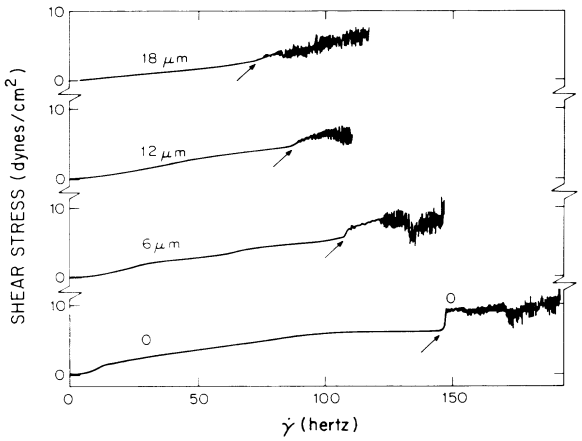

FIG. 3. *In situ* measurement of the stress vs rate on the outer wall of the Couette cell for different electrolyte concentrations in micromoles HCl. For 18 μM HCl, the sample is melted in the absence of any shear.

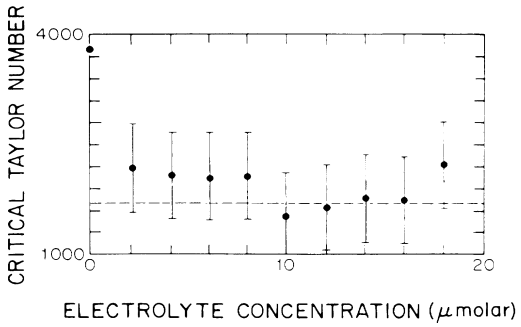

FIG. 4. Critical Taylor number vs electrolyte concentration from a set of stress-rate curves as in Fig. 3.

cell. Briefly, a thin disk of $\sim$0.5-cm diameter is placed in a hole of $\sim$0.51-cm diameter in the outer cylinder. The disk is flush with the inner surface to $\sim$0.05 cm and is supported on a thin rod which goes through a membrane to a chamber outside the cell. The chamber is filled with a liquid to equalize the pressure across the membrane. The rod is attached to a mirror mounted on a torsion fiber. A shear stress at the wall of the Couette cell causes a displacement of the inner disk, which in turn displaces the mirror. This displacement is measured by monitoring of the reflection of a laser with a position-sensitive photodiode. The apparatus is calibrated by measurements on Newtonian fluids with well-characterized viscosities.

Typical examples of the curves of stress versus rate obtained are shown in Fig. 3 for samples with varying electrolyte concentration. At low $\dot{\gamma}$ the shear stress increases smoothly with the shear rate corresponding to the flowing solid. Then a sharp increase of the shear stress indicates the onset of the Taylor–shear-melting transition. Note that this jump is much more abrupt than that seen when shear melting occurs without the Taylor rolls (Fig. 1) or when a Taylor instability occurs in a Newtonian fluid, when there is simply a slope change, as seen for the liquid sample (Fig. 3, 18 μM). This demonstrates that the shear stress (and hence viscosity) is indeed higher at Ω_c, as required for T_c. Note also that the "wavy Taylor" instability characterized by the oscillations in the curves at high $\dot{\gamma}$ occurs at $\sim 1.16\Omega_c$. This is the same factor as for conventional fluids in this geometry, suggesting that the radial velocity is small at the onset of the Taylor instability as it is for conventional Taylor rolls, and as observed visually. This also adds credence to the description of the Taylor–shear-melted liquid as a nearly Newtonian fluid with a high viscosity.

The observation that the radial and axial velocities in the Taylor rolls are small at the onset shows that the total local shear rate in the Taylor–shear-melted liquid is essentially that determined by the rotation frequency of the inner cylinder. Since this shear rate is $\sim$2–3 times less than that required for shear melting when the outer cylinder is rotating, we have demonstrated that the shear rate is not the universal control parameter for determining the shear-melting transition. This suggests that the theories for this transition need revision.

Without an adequate theory of the shear-melting transition we cannot give detailed explanation for the combined Taylor–shear-melting transition. However, we can phenomenologically predict the rotation rate at which the transition occurs. To obtain the appropriate value of the viscosity of the liquid phase just above the transition, we use the stress measured just above the transition and divide by the rate at the transition. This results in the expected value for T_c for our geometry, as shown in Fig. 4 for the data from Fig. 3. (We do not yet understand the anomalously high value which occurs in most freshly deionized samples in the absence of added electrolyte.) Moreover, the shear stress at the transition measured in the Couette cell is, within our experimental calibration error ($\pm$20%), the same stress at shear melting as we observe in the Zimm viscometer without the Taylor instability. Thus we can measure the critical shear stress from data of the sort shown in Fig. 1, define an effective viscosity at the transition, $\nu_{\text{eff}} = \sigma_{\text{sm}}/\dot{\gamma}_{\text{T-sm}}$, and correctly predict the combined Taylor–shear-melting transition at an Ω_c given by $T_c = \Omega_c{}^4 R^3/\sigma_{\text{sm}} = 1700$. Note that $\sigma_c \sim \sigma_{\text{sm}}$ in Fig. 1. This observation suggests that the shear-melting instability may be controlled by the stress rather than the rate when different flow configurations are used. Any model for the shear melting must properly account for this.

[a]Permanent address: Physique de la Matiére Condensée, College de France, 11, place Marcelin-Berthelot, 75231 Paris

Cedex 05, France.

[1]P. Pieranski, Contemp. Phys. **24**, 25 (1983); W. van Megen and I. Snook, Adv. Colloid Interface Sci. **21**, 119 (1984).

[2]P. M. Chaikin, J. M. di Meglio, W. D. Dozier, H. M. Lindsay and D. A. Weitz, in "Physics of Complex and Supermolecular Fluids," edited by S. Safron and N. Clark (Wiley, New York, to be published).

[3]B. J. Ackerson and N. A. Clark, Phys. Rev. Lett. **46**, 123 (1981).

[4]R. L. Hoffman, Trans. Soc. Rheol. **16**, 155 (1972), and J. Colloid Interface Sci. **46**, 491 (1974).

[5]B. J. Ackerson and N. A. Clark, Phys. Rev. A **30**, 906 (1984); N. A. Clark, B. J. Ackerson, and T. W. Taylor, J. Phys. (Paris), Colloq. C3, **46**, 137 (1985).

[6]S. Ramaswamy and S. R. Renn, Phys. Rev. Lett. **56**, 945 (1986).

[7]H. M. Lindsay and P. M. Chaikin, J. Chem. Phys. **76**, 3774 (1983).

[8]H. M. Lindsay and P. M. Chaikin, J. Phys. (Paris), Colloq. **46**, C3-269 (1985).

[9]G. I. Taylor, Phil. Trans. Roy. Soc. London, Ser. A **223**, 223 (1983).

[10]D. A. Weitz, W. D. Dozier and P. M. Chaikin, J. Phys. (Paris), Colloq. **46**, C3-257 (1985).

[11]M. Jorand, F. Rothen, and P. Pieranski, J. Phys. (Paris), Colloq. **46**, C3-245 (1985) and in Ref. 2.

[12]M. Joannicot and P. Pieranski, J. Phys. (Paris), Lett. **46**, L91 (1985).

[13]S. Chandrasekhar, *Hydrodynamic and Hydromagnetic Stability* (Dover, New York, 1961).